Aust. J. Phys., 1980, 33, 139–57

Galactic Plane H_2O Masers: A Southern Survey

R. A. Batchelor,[A] *J. L. Caswell,*[A] *W. M. Goss,*[A,B] *R. F. Haynes,*[A] *S. H. Knowles,*[A,C] *and K. J. Wellington*[A]

[A] Division of Radiophysics, CSIRO, P.O. Box 76, Epping, N.S.W. 2121.
[B] Present address: Kapteyn Astronomical Institute, University of Groningen, Postbus 800, Groningen, Netherlands.
[C] Present address: U.S. Naval Research Laboratory, Washington, D.C., 20375, U.S.A.

Abstract

An extensive 22 GHz survey of H_2O masers has been made with the Parkes 64 m radio telescope. We present data here for 68 sources, of which almost one-half were discovered in the present series of observations. The telescope beamsize, 100″ arc to half-power, has enabled us to improve the position measurements of most of the known sources and in a few cases has allowed us to resolve a 'source' into several spatially separated components. The wide velocity coverage of our observations (>200 km s^{-1}) has led to the discovery of several interesting new high-velocity features. In addition to details for each source, the general properties of the sample are discussed. In the typical interval of 8 months between successive observations, the peak intensity of many sources varied only slightly (by less than a factor of 2); a few sources, however, showed more dramatic variations.

1. Introduction

It is now recognized that water vapour masers have a role to play in the investigation of physical conditions in regions of star formation. Indeed, they may be the most sensitive indicator of regions of recent star formation. Our understanding of these objects is far from complete: there is no satisfactory detailed explanation for the extreme high-velocity emission from some of the masers, nor for the often dramatic time variability of the intensity.

In several previous investigations, a few objects (notably W49 and Orion A) have been singled out for detailed study, for example, by very long baseline interferometry techniques and frequent monitoring of the intensity variations with time. Even for these sources, however, many problems remain unsolved, and the compilation of a much larger sample for further study is clearly desirable. A knowledge of the total number of H_2O masers in our Galaxy, together with the typical power output, can itself be an important constraint on models to account for the masers.

In this work we have been particularly concerned with compiling an extensive catalogue of H_2O masers in that large part of the galactic plane which is observable only from southern hemisphere sites, i.e. declinations south of $-30°$, corresponding to galactic longitudes between 250° and 360°. However, our survey is by no means a *complete* search of this large region, since the observing time required would be prohibitive with our small beamsize; the positions which we have investigated are the sites of type I OH masers. We also present new observations of previously known H_2O masers discovered either by the Itapetinga telescope (Kaufmann *et al.* 1976; subsequently referred to as K+ 76) or in our earlier Parkes searches; thus the catalogued sources in Table 2 given here are now covered by a homogeneous set

of observations. Our subsequent discussion covers details of the more interesting individual sources, together with the overall properties of the whole group.

While this study was in progress, a similar survey in the northern hemisphere was commenced (Genzel and Downes 1977*a*; subsequently referred to as GD 77*a*). The two surveys are complementary in sky coverage and the overlap region contains 15 sources in common. Observations of these sources permit some interesting comparisons since in many cases we have made measurements both before and after GD 77*a* observations.

Table 1. Observing sessions at 22 GHz for H_2O masers

Date of session	Ratio S/T (Jy K^{-1})	Beam-size (″ arc)	Velocity coverage (km s^{-1})	Comments
1975 Dec.	23[A]	180	230	See Caswell *et al.* (1976)
1976 Apr.	8	100	?	Mainly polarization; see Knowles and Batchelor (1978)
1976 Aug.	8	100	230	Some sources discussed by Goss *et al.* (1977)
1976 Nov.	8	100	215	Mainly stars (R. F. Haynes, unpublished data)
1977 May	8	100	215	

[A] Illumination of only central 17 m of dish, compared with 37 m in other sessions.

2. Equipment and Observations

Details of the five observing sessions are listed in Table 1 together with references to some preliminary data; the equipment used has already been described in the earlier publications and will be summarized briefly here.

In the first observing session only a 17 m diameter portion of the Parkes 64 m dish was illuminated whereas in the remaining sessions 37 m was illuminated. The 22 GHz cooled mixer receiver yielded a system temperature (SSB) of between 600 and 1000 K. After a typical observation comprising a 10 min integration on source and a 10 min comparison spectrum, the r.m.s. noise when observing with an effective resolution of 40 kHz ($\equiv 0{\cdot}53$ km s^{-1}) was $\sim 0{\cdot}3$ K ($\equiv 3$ Jy for 37 m illumination). The autocorrelation spectrometer was used to analyse two 10 MHz bandwidths which overlapped by 3 or 4 MHz to give a total velocity coverage of 230 or 215 km s^{-1}. The flux density scale is relative to Jupiter, assumed to have a brightness temperature of 140 K, uniform over the optical disc. Atmospheric attenuation during good observing conditions was measured to be between 10% and 12% at the zenith and this value was assumed when no direct measurements were made; the source flux densities are corrected to the equivalent 'above the atmosphere' values.

Apart from a study of the polarization of H_2O masers (reported elsewhere by Knowles and Batchelor 1978), the observations were all made with a linearly polarized feed, with its $\boldsymbol{E}$ plane aligned vertically. In the following discussion of source intensity variations, it is assumed that any linear polarization is small; this is justified by the available polarization information (Knowles and Batchelor 1978).

The H_2O sources observed were as follows.

(i) New sources which we discovered by searching at the positions of OH masers: many of these OH masers were found in an extensive new survey soon to be published (Caswell *et al.* 1980).

(ii) Sources recently discovered by K+76 and Kaufmann *et al.* (1977; subsequently abbreviated to K+77) at the Itapetinga observatory: for these sources we have determined more accurate positions and investigated a larger range in velocity.

(iii) Other previously reported sources: these were observed in order either to monitor intensity variations or to improve the positional accuracy.

Our positional accuracy is limited by the pointing errors of the telescope ($\sim 12''$ arc (r.m.s.) in each coordinate after correcting for systematic errors), although there is an additional uncertainty for weak sources where the signal to noise ratio is low. Positions were determined from spectra taken at a grid of points around the source; the accuracy of *relative* positions of strong components within the beam is almost an order of magnitude better than the absolute accuracy.

3. Results

A summary of the results is presented in Table 2. This catalogues the position of each source (columns 3 and 4), the velocity of the most prominent feature (column 5), the peak intensities of this feature as measured in our observations (column 7) and the epochs of these measurements (column 8: usually we have made at least two observations; where more have been made we have added 'etc.'). A discovery epoch is printed in bold type.

For sources showing a single main feature we quote in Table 2 (column 6) an approximate width to half intensity; where the velocity structure is more complex it is necessary to consult Figs 1–4 below and/or the following notes. In cases where different velocity components emanate from slightly different positions, this is also discussed in the notes. Selected references to earlier work are given (column 9) but, if the position previously had a large uncertainty or the velocity structure was markedly different from its present appearance, comparisons should be treated with caution since there may be more than one source present. Note that previous source designations usually quote galactic coordinates to 1/10 degree; however, the masers are essentially point sources and, in view of the accuracy of positions now achieved and the existence of close pairs of sources, we have chosen to quote (in column 1) galactic names to the nearest 1/100 degree.

For each source we have indicated in Table 2 the presence or absence of a nearby OH maser (column 10); this is not intended to imply an intimate association between OH and H_2O sources, although the separations are generally less than $\sim 1'$ arc. The OH data are taken principally from our own observations, although similar data are available for the northern sources in several miscellaneous publications; new OH results obtained at Parkes and as yet unpublished are indicated by (P) in column 10.

In the remarks column of Table 2 we draw attention to sources of particular interest, e.g. those exhibiting features spread over a wide range in velocity, those showing two or more spatially separated features and those showing dramatic variability (an order of magnitude) in the peak intensity. These sources, together with the generally more intense ones, will form a particularly valuable sample for future monitoring.

We have omitted from the results our data on some well-known northern sources since these are better assessed elsewhere in the context of the large body of data already published (earlier data on Sgr B2, H_2O $10{\cdot}6-0{\cdot}4$, W49 and W51 are given by GD 77*a*).

1980AuJPh..33..139B

Table 2. Catalogue of southern H_2O masers

(1) Galactic coordinates (H_2O)	(2) Name	(3) Position (1950)[A] R.A. h m s	(4) Dec. ° ′ ″	(5) Velocity V (km s^{-1})	(6) Width ΔV (km s^{-1})	(7) Intensity S (Jy)	(8) Observation dates[B]	(9) H_2O refs[C]	(10) OH?	(11) Remarks
208·99−19·39	Orion A	[05 32 46·7	−05 24 28]	+11	See text	5500	77.5.25 etc.	GD77*b*	Yes	High velocity; displaced position
188·94+0·89		06 05 53·7	+21 39 09	−5	~1; see text	13; 40	**76.8.9**; 77.5.22	—	Yes	
192·60−0·05	S255/7	[06 09 58	+18 00 02]	+9	~1·5; see text	115	76.8.9	GD77*a*	Yes	
196·46−1·68	S269	[06 11 48	+13 50 24]	+17	~1; see text	~90	76.8.9	GD77*a*	Yes	
267·94−1·06	RCW 38	08 57 21·7	−47 19 04	−3	Fig. 1	20; 35	76.8.10; 77.5.21	K+76; K+77	No	Possibly two or more positions; wide velocity spread
284·36−0·42	RCW 49	10 22 20·9	−57 37 48	+7	~4	340	77.5.22	SS77	No (P)	
285·26−0·05		10 29 36·8	−57 46 40	+3	Fig. 1	560; 980	76.8.10; 77.5.24 etc.	CBHH	Yes	Wide velocity spread
291·27−0·71		11 09 42·0	−61 01 55	−123	7	250; 270	76.8.8; 77.5.23	G+77	No	Intense high-velocity emission; displaced position
291·57−0·43		11 12 54·0	−60 52 57	+14	Fig. 1	360; 260	75.12.10; 76.8.10 etc.	CBHH	Yes	
300·97+1·14		12 32 00·2	−61 23 44	−63	Fig. 1	90	**77.5.25**	—	Yes	
305·20+0·21		13 07 59·9	−62 18 50	−41	Fig. 1	150	76.11.26	K+76; K+77	Yes	
305·36+0·21		13 09 21·2	−62 18 02	−37	Fig. 1	60; 70	76.8.10; 77.5.23 etc.	C+76	No	High-velocity emission; displaced positions
305·36+0·15		13 09 21·0	−62 21 43	−37	Fig. 1	40; 70	76.8.6; 77.5.23 etc.	C+76	Yes	Highly variable
316·77−0·02		14 41 10·4	−59 35 30	−39	~2	40; 25	**76.8.10**; 77.5.25	—	Yes	
316·81−0·06		14 41 36·4	−59 36 53	−46	~3	290; 280	76.11.28; 77.5.25	K+76; K+77	No	
324·20+0·12		15 29 01·2	−55 46 12	−93	~1	40; 40	**76.8.5**; 77.5.20	—	Yes	
326·64+0·61		15 40 42·6	−53 56 29	−38	~2	780	77.5.24	K+76; K+77	No	
327·12+0·51		15 43 42·9	−53 43 48	−84	~1; see text	20	**77.5.26**	—	Yes (P)	
327·29−0·57		15 49 12·5	−54 28 12	−58	Fig. 1	1500; 1040	75.12.14; 76.8.10 etc.	CBHH; G+76	Yes	High-velocity emission
327·39+0·45		15 45 27·4	−53 36 25	−79	~2·5	30; 30	76.8.5; 77.5.21	—	Yes (P)	
328·30+0·43		15 50 15·3	−53 02 46	−95	~1	40	**76.8.8**	—	Yes (P)	
329·18−0·32		15 57 58·1	−53 03 38	−47	~1	50	**76.8.5**	—	Yes	
329·40−0·46		[15 59 41·1	−53 01 33]	−76	~1	⩾25; ~10	**76.8.5**; 77.5.22	—	Yes	
330·88−0·36		16 06 30·0	−51 58 14	−52	Fig. 2	320; 70	**75.12.15**; 76.8.10 etc.	C+76; K+76; K+77	Yes	Highly variable

1980AuJPh..33..139B

330·95−0·19		16 06 03·4	−51 47 30	−90	Fig. 2	460; 260	75.12.12; 76.8.10 etc.	CBHH etc.	Yes	High velocity
331·13−0·25		16 07 11·0	−51 42 53	−81	Fig. 2	30	**76.8.8**	—	Yes (P)	
331·51−0·10		16 08 21·0	−51 21 11	−95	Fig. 2	4300; 2100	75.12.10; 76.8.10 etc.	CBHH	Yes	High velocity
332·65−0·63		16 15 55·7	−50 56 48	−44	∼2·5	30	77.5.22	K+76; K+77	No	
333·23−0·05		16 16 02·0	−50 07 50	−90	Fig. 2	150	76.8.6	K+76; K+77	Yes	
333·13−0·43		16 17 12·6	−50 28 18	−44	Fig. 2	80; 115	75.12.11; 76.8.10 etc.	CBHH etc.	Yes	
333·60−0·22		16 18 24·5	−49 59 08	−52	Fig. 2	100; 100	75.12.13; 76.8.10 etc.	CBHH etc.	Yes	
335·78+0·17		16 26 03·1	−48 09 44	−59	∼2; see text	25; 50	**76.8.9**; 77.5.23	—	Yes (P)	
336·99−0·03		16 31 52·5	−47 25 08	−120	Fig. 3	250	**76.8.9**	—	Yes (P)	
337·40−0·40		16 35 08·1	−47 22 23	−43·5	∼1; see text	540; —	**75.12.14**; 76.8.10	C+76	Yes (P)	Highly variable
337·61−0·06		16 34 29·1	−46 59 17	−48	∼5	15; 15	**76.8.7**; 77.5.22	—	Yes (P)	
337·71−0·05		16 34 47·4	−46 54 13	−44	∼10	30	**76.8.8**		Yes	Single feature, unusually broad
337·86+0·26		16 34 03·9	−46 34 54	−86	∼2	70; 30	**75.12.13**; 77.5.26	C+76	Yes	OH/IR star?
337·91−0·47		16 37 25·9	−47 02 06	−39	Fig. 3	210; 90	75.12.13; 76.8.6 etc.	CBHH etc.	Yes	
337·99+0·14		16 35 07·1	−46 34 11	−38	Fig. 3	200	**76.8.10**	—	Yes (P)	High-velocity feature
338·27+0·54		16 34 28·7	−46 05 19	−60	Fig. 3	—; 30	**76.8.7**; 77.5.22	—	Yes (P)	
338·92+0·56		16 36 54·0	−45 36 05	−75	Fig. 3	50; —	76.8.10; 77.5.24	K+76; K+77	Yes	High velocity; displaced position
339·62−0·12		16 42 28·6	−45 31 33	−35	∼1	15; 65	**76.8.6**; 77.5.22	—	Yes	
340·06−0·25		[16 44 39·0	−45 16 26]	−52	∼2	7; <7	**76.8.9**; 77.5.21	—	Yes	
343·12−0·06		16 54 42·8	−42 47 49	−34	Fig. 3	100	**77.5.25**	—	Yes (P)	
345·41−0·94		17 06 02·3	−41 31 44	−22	∼1	30; ≤20	**76.8.7**; 77.5.24	K+74?	Yes	
345·51+0·35		17 00 53·6	−40 40 02	−28	1·5	530	76.8.8	K+76; K+77	Yes	
345·69−0·09		17 03 19·7	−40 47 31	−9	Fig. 3	590; 290	75.12.12; 76.8.9 etc.	CBHH etc.	Yes	
348·73−1·04		17 16 39·7	−38 54 17	−11	Fig. 3	390	76.8.11	K+76; K+77	Yes	High velocity
349·09+0·11		17 12 58·4	−37 56 21	−81	Fig. 4	80; 370	75.12.11; 76.8.10	C+76; (K+77)	Yes	
351·16+0·70	NGC 6334B/S	17 16 34·5	−35 54 44	−6	∼2·5	5; 20	76.8.8; 77.5.24 etc.	G+77	Yes	High velocity; highly variable
351·41+0·64	NGC 6334A/N	[17 17 32·5	−35 44 13]	−9	Fig. 4	3200; ?	76.8.11; 77.5.24 etc.	G+76	Yes	High velocity

[A,B,C] See footnotes at end of table.

1980AuJPh..33..139B

Table 2 (*Continued*)

(1) Galactic coordinates (H_2O)	(2) Name	(3) Position (1950)[A] R.A. h m s	(4) Dec. ° ′ ″	(5) Velocity V (km s^{-1})	(6) Width ΔV (km s^{-1})	(7) Intensity S (Jy)	(8) Observation dates[B]	(9) H_2O refs[C]	(10) OH?	(11) Remarks
353·41−0·36		17 27 06·5	−34 39 41	−14	Fig. 4	18; 45	**76.8.8**; 77.5.24	—	Yes	
356·64−0·33		17 35 26·1	−31 56 00	−10	~3; see text	20	**77.5.26**	—	Yes (P)	IR star?
0·54−0·85		17 47 03·2	−28 53 54	+18	Fig. 4	25; 60	76.11.28; 77.5.22	K+76; K+77; KM; GD77*a*	Yes	Wide velocity spread
5·89−0·40	W28 (A2)	17 57 28·7	−24 03 53	+7	~1; see text	200; 25	75.12.13; 76.4.5 etc.	C+76; GD77*a*	Yes	High-velocity features; highly variable
12·21−0·11		18 09 42·8	−18 25 20	+23	~1; see text	85; 160	**76.8.10**; 77.5.23	G+77; GD77*a*	Yes	Wide velocity; displaced positions
12·68−0·18	W33B	18 10 58·3	−18 02 43	+58	~2	270	75.12.10	GD77*a*	Yes	
12·91−0·26	W33A	[18 11 44·6	−17 52 57]	+37	~2	10	77.5.26	GD77*a*	Yes	
14·17−0·06		18 13 32·9	−16 40 43	+61	Fig. 4	15; 30	**76.8.7**; 77.5.23	—	Yes	
14·99−0·69	M17(1)	[18 17 29·8	−16 15 37]	−4	~3; see text	50	76.8.7	GD77*a*; LDGW76	?	Highly variable
15·02−0·67	M17(2)	18 17 27·4	−16 13 20	+15	~1; see text	140; 30	75.12.10; 76.8.11	JSB73; C+76; GD77*a*	Yes	High velocity; displaced position; highly variable
19·60−0·23		18 24 48·4	−11 58 45	+44	~5; see text	60; 60	75.12.12; 76.8.10	C+76; GD77*a*	Yes	
24·79+0·08		18 33 30·9	−07 14 27	+110	~5	130; 70	75.12.11; 76.8.10	C+76; GD77*a*	Yes	
30·81−0·06		18 45 10·1	−01 58 00	+82	~1; see text	300	**75.12.12**	C+76; GD77*a*	Yes	Wide velocity spread
31·21−0·18		[18 46 20·7	−01 40 10]	−39	~2	⩾15	**76.8.7**	—	Yes	No measurement of accurate position
34·25+0·16		18 50 44·4	+01 11 13	+60	~1·5; see text	400; 250	75.12.14; 76.8.9	CBHH; GD77*a*	Yes	High-velocity feature
35·20−0·74		18 55 40·8	+01 36 30	+33	~1	65; 30	**76.8.9**; 77.5.23	—	Yes	
43·80−0·12		19 09 30·5	+09 30 50	+40	~3; see text	330; 280	**76.8.9**; 77.5.23	GD77*a*	Yes	High-velocity feature

[A] Positions are as measured at Parkes unless enclosed in square brackets (see the source notes in Section 3 for these cases).

[B] Dates of discovery observations are shown in bold.

[C] Reference abbreviations: GD77*b*, Genzel and Downes (1977*b*); GD77*a*, Genzel and Downes (1977*a*); K+76, Kaufmann *et al.* (1976); K+77, Kaufmann *et al.* (1977); SS77, Scalise and Schaal (1977); CBHH, Caswell *et al.* (1974); G+77, Goss *et al.* (1977); C+76, Caswell *et al.* (1976); G+76, Goss *et al.* (1976); K+74, Kaufmann *et al.* (1974); KM, Knapp and Morris (1976); LDGW76, Lada *et al.* (1976); JSB73, Johnston *et al.* (1973).

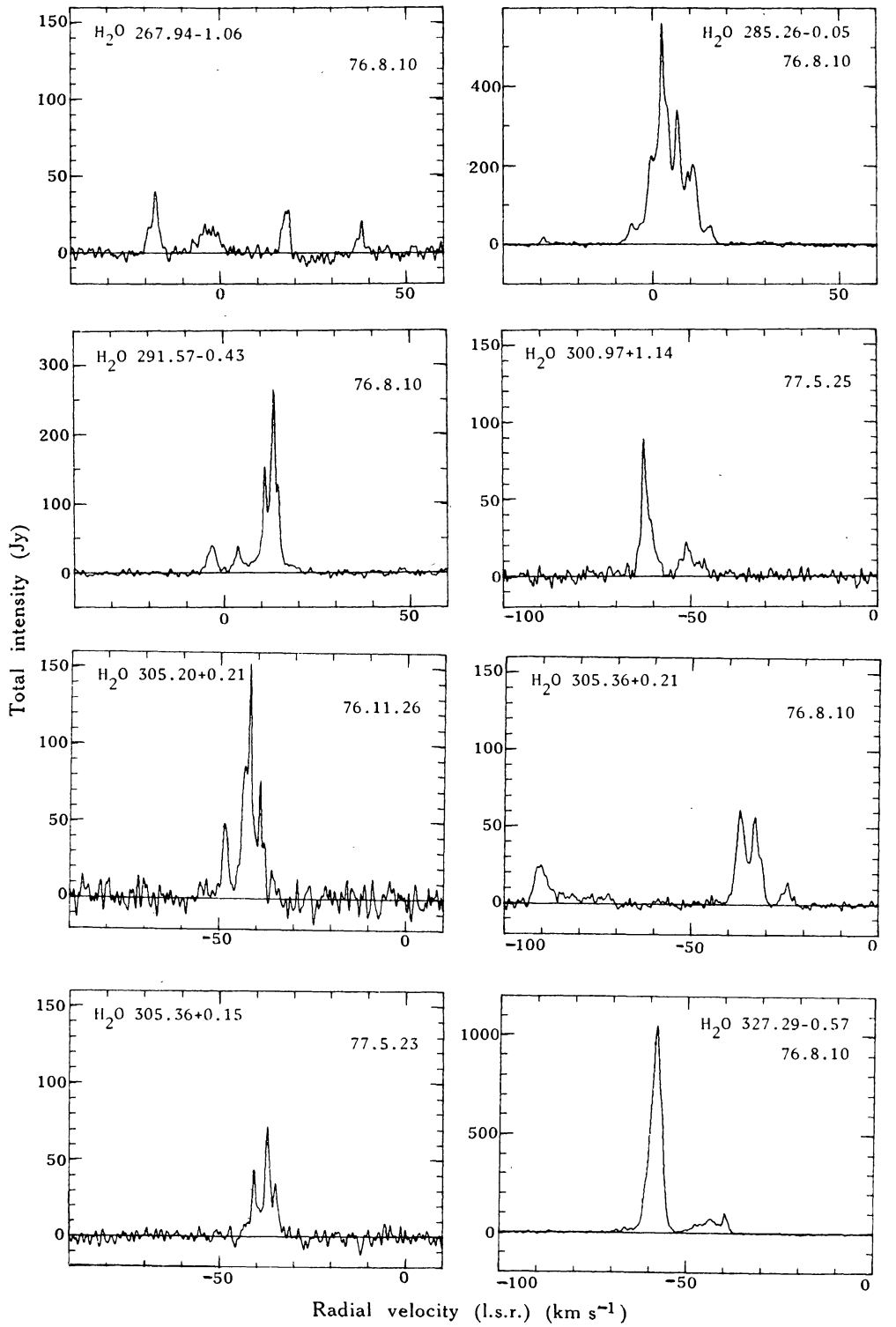

Figs 1–4. Spectra of H_2O masers. The source names and observing dates are shown within each frame. The velocity resolution is 0·53 km s^{-1} (≡ 40 kHz).

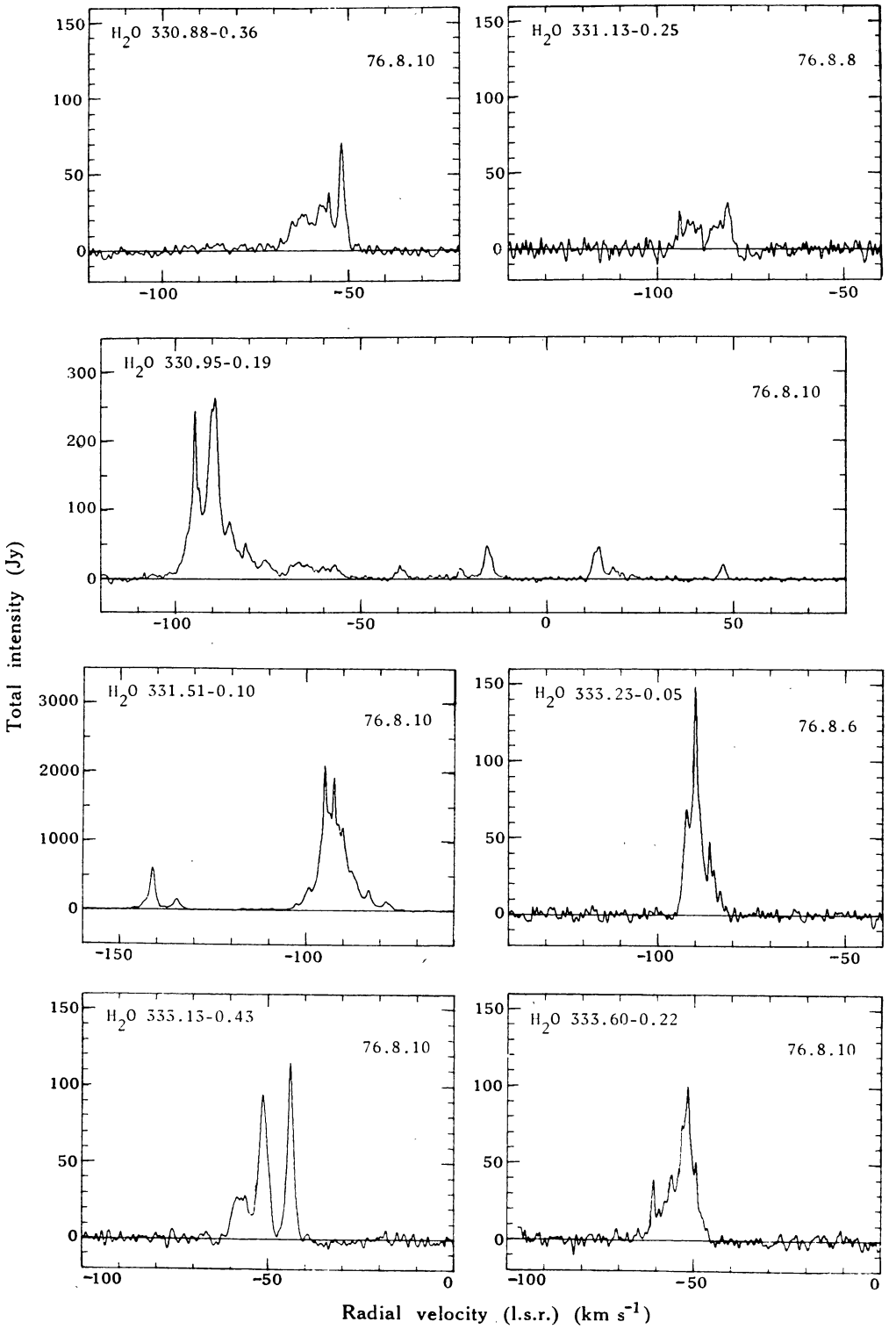

Fig. 2

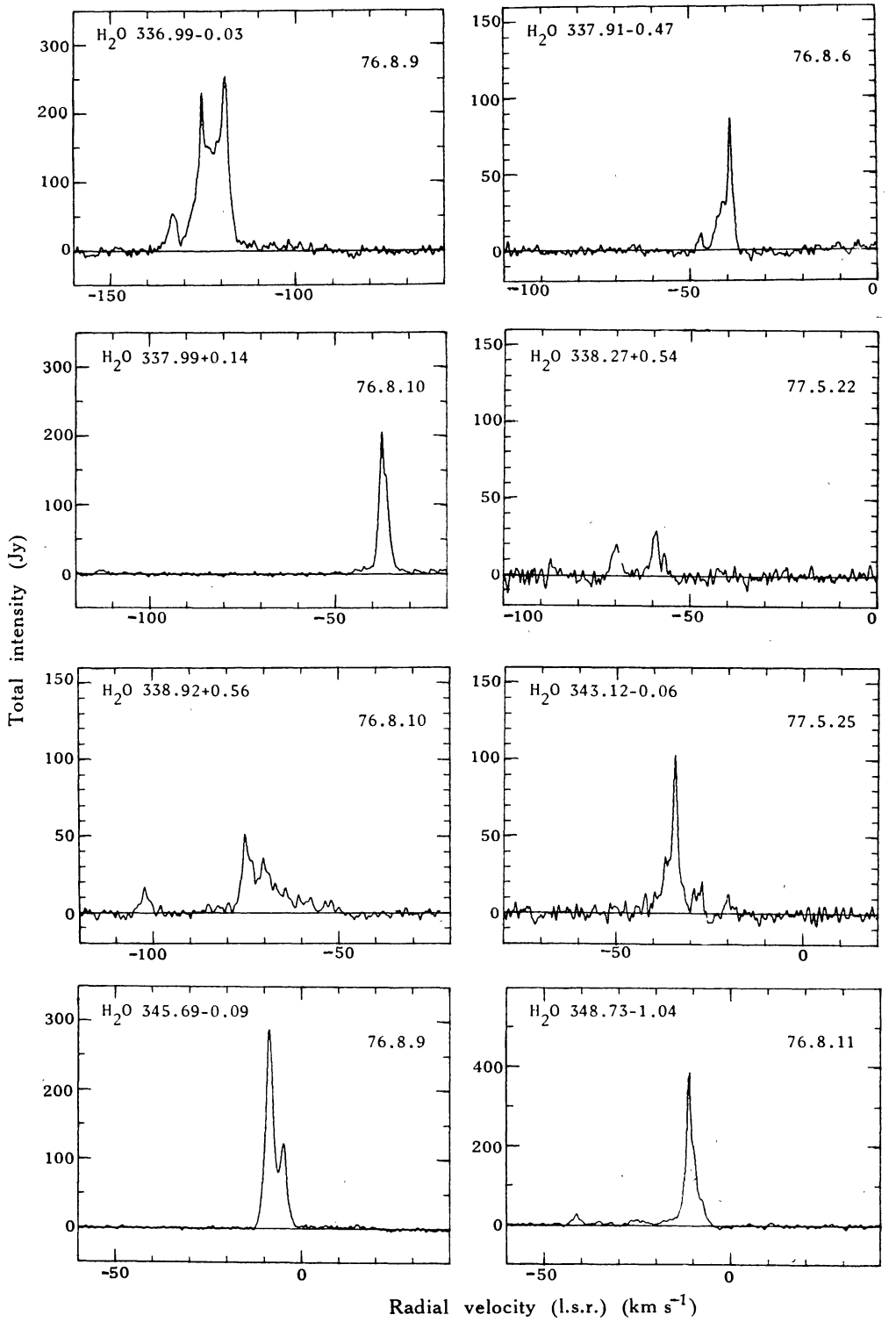

Fig. 3

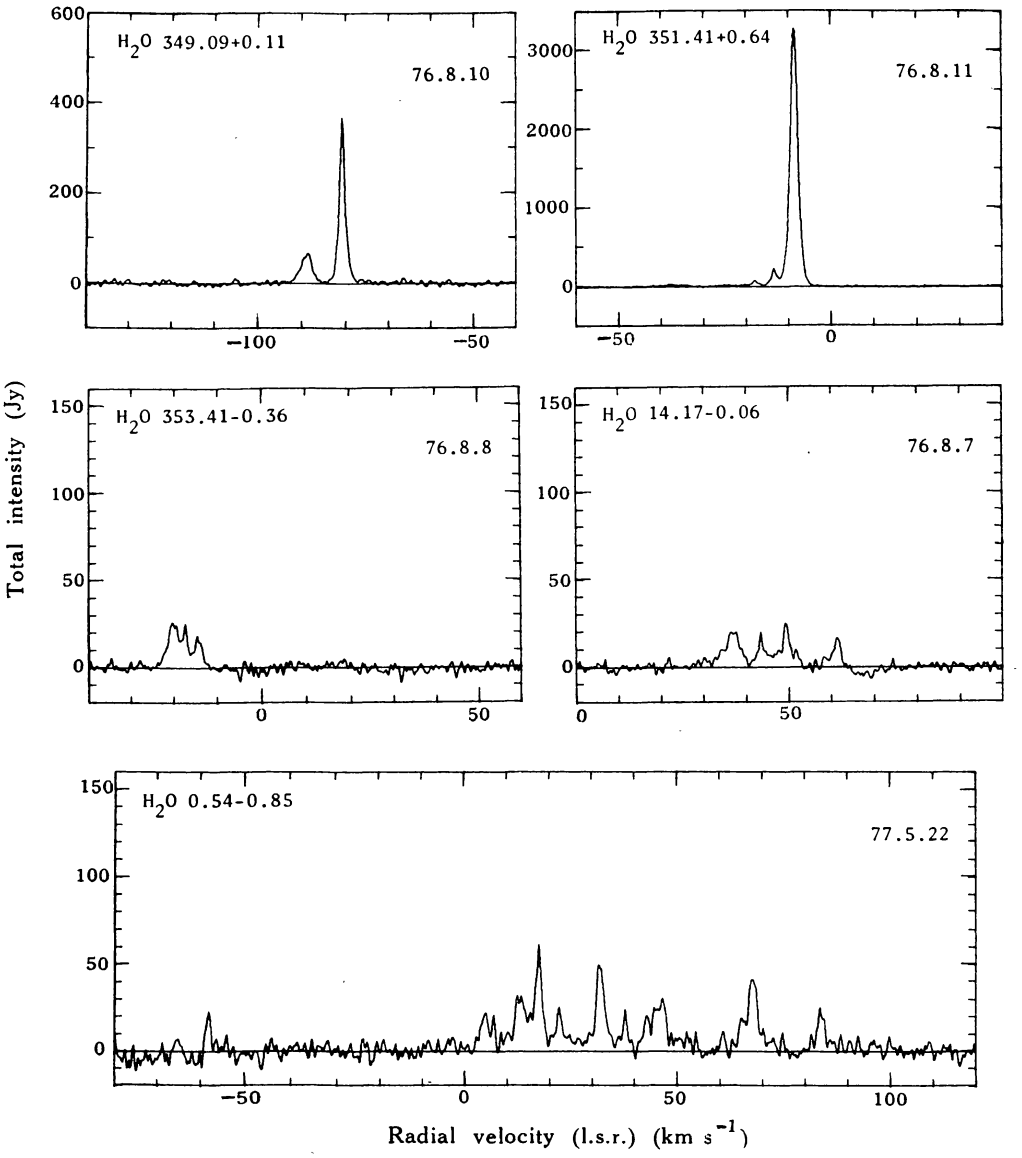

Fig. 4

Figs 1–4, which show spectra of many of the sources, do not cover the full velocity range of our observations; generally the complete observations extend approximately ± 110 km s^{-1} relative to the main emission velocity with an r.m.s. noise level similar to that seen at the centre of the profile (or usually ~ 3 Jy).

The subsequent notes give more detailed comments, in particular comparing data at different epochs, from both our own and other observations.

H_2O 208·99 − 19·39 (Orion A). This source is extensively discussed by Genzel and Downes (1977*b*); Table 2 quotes 'position A' from their results. Parkes maps at regular intervals (1975 May, see Goss *et al.* 1976; 1976 April, see Knowles and Batchelor 1978; 1977 May, a grid of points observed during the current set of

observations) and the more accurate Genzel and Downes (1977*b*) map of 1976 December are generally in good agreement. An interesting change in the 1977 May data is that high-velocity features at $V = +51$ and $+69$ km s^{-1} are both a factor of ~ 4 stronger than in 1976 December; both features are 'narrow band' and relatively isolated in velocity so that they appear to be reliably identified with features in the Genzel and Downes spectra; but the 1977 May grid of observations reveals that whereas this is probably true of the $+51$ km s^{-1} feature, the $+69$ km s^{-1} feature is at a completely different and isolated position, i.e. $\sim 27''$ arc to the north-west of the Genzel and Downes position.

H_2O 188·94+0·89. This is a new source near the position of a 1665 MHz OH source (Parkes, unpublished data). The main feature, at $V = -5$ km s^{-1}, increased from 13 to 40 Jy between 1976 August and 1977 May; a 10 Jy feature at $V = +8$ km s^{-1} was present on both occasions.

H_2O 192·60−0·05. The three-peaked structure in 1976 August was similar to that in 1977 January (GD 77*a*) but stronger by $\sim 50\%$. We did not measure the position (see GD 77*a*).

H_2O 196·46−1·68. The main feature increased in intensity only slightly from 1976 August to 1977 February (GD 77*a*) with some change in the weaker emission. We did not measure the position (see GD 77*a*).

H_2O 267·94−1·06. In 1976 August (Fig. 1) four features were seen; all except the $+37$ km s^{-1} feature were detected again in 1977 May. We quote a mean position but there was some indication that the features were spatially separated by up to $30''$ arc. Two of the features on the discovery profile (K+ 76, K+ 77) coincide with features in Fig. 1. No nearby OH maser has been detected (Caswell *et al.* 1977).

H_2O 284·36−0·42. The intensity of this strong single feature in 1977 May was very slightly weaker than at the discovery epoch, 1977 February (Scalise and Schaal 1977). Our search for OH maser emission (1977 April) showed none at 1665 MHz, the upper limit being 0·5 Jy in each sense of circular polarization.

H_2O 285·26−0·05. Over several years this strong source has consistently shown about five features, the intensity of the strongest being between 500 and 1000 Jy. In the profile of 1976 August (Fig. 1) a 'high-velocity' feature at $V = -30$ km s^{-1} is seen; in 1975 December a feature at $V = +21$ km s^{-1} was seen; neither was detected in 1977 May, although the main features (between -4 and $+15$ km s^{-1}) were similar.

H_2O 291·27−0·71. This unusual source has a broad high-velocity feature at $V = -123$ km s^{-1} (Goss *et al.* 1977) with an intensity greater (by a factor ~ 3) than the emission in the HII region velocity range ($V = -32$ km s^{-1}), and is spatially displaced from it by $44''$ arc. Our latest observations (1977 May) reveal some variation in velocity structure but the peak intensities show no marked change, indicating that the phenomenon is quite long-lived (>1 yr). No nearby OH emission has been detected (Caswell *et al.* 1977). Highly blue-shifted H_2O masers (similar to this source) were found in association with two Herbig–Haro objects by Rodriguez *et al.* (1978; see also the notes to H_2O 351·16+0·70 below). Prompted by this, we inspected the SRC(J) plate of the Southern Sky survey at the position of H_2O 291·27−0·71 and

found a knot of optical emission, $\sim 6'' \times 18''$ arc essentially coincident with the H_2O maser; a spectroscopic investigation is needed to ascertain whether this may be a Herbig–Haro object.

H_2O 291·57−0·43. Since its discovery in 1971 May, the velocity structure has varied but the peak intensity has not changed by more than a factor of 2. The most recent profile is shown (Fig. 1) and has the best sensitivity obtained to date.

H_2O 305·20+0·21. Fig. 1 shows more detail than the discovery profile of K+ 77, but the peak intensity remains comparable (taking into account the different velocity resolution).

H_2O 305·36+0·21. Fig. 1 shows that, in addition to main features near $V = -35$ km s^{-1}, there is quite strong emission at the high velocity of -90 km s^{-1}. In 1975 December the main features were somewhat stronger than in 1976 August and the high-velocity emission was at $V = -82$, -92, -102 and -106 km s^{-1}. In 1977 May the emission resembled that in 1976 August with the addition of a strong (60 Jy) feature at $V = -74$ km s^{-1}. The position quoted is for the emission at -33 km s^{-1}; the high-velocity emission is displaced 50″ arc south and about 10″ arc west, whereas the -37 km s^{-1} emission lies between these positions and may indicate blending of features from the two positions. The high-velocity emission has varied more than the low-velocity features.

H_2O 305·36+0·15. Several features are seen in Fig. 1; their intensities are much lower than the peak of 550 Jy observed in 1973 June and none of them coincides with it in velocity.

H_2O 316·81−0·06. Our observations (1976 November and 1977 May) of this strong source discovered by K+ 76 and K+ 77 showed essentially no change compared with the discovery profile. Weaker emission extends from the main feature (at $V = -46$ km s^{-1}) to $V = -30$ km s^{-1}.

H_2O 326·64+0·61. Our measurement (1977 May) shows a strong single feature at $V = -38$ km s^{-1}, presumably corresponding to the feature first reported by K+ 76 and K+ 77. The feature is much stronger in our observations, a fact partly attributable to the displaced position of these K+ observations (1976 May), but a real intensity increase of ~ 3 times is nonetheless indicated. The other features reported by K+ had fallen below our detection limit (<10 Jy).

H_2O 327·12+0·51. We discovered this H_2O source in the direction of a new OH maser (Caswell *et al.* 1980); the H_2O profile shows a main feature at -84 km s^{-1} and a weaker feature at -78 km s^{-1}.

H_2O 327·29−0·57. Since 1973 June (Caswell *et al.* 1974) this has remained one of the strongest H_2O sources; the high-velocity features detected in 1975 May (Goss *et al.* 1976) were not detected in 1976 August, but the overall appearance (Fig. 1) remains similar though weaker by a factor of ~ 2.

H_2O 329·40−0·46. The position quoted is the discovery position where there is an OH source (Caswell and Haynes 1975). In 1977 May the H_2O line intensity had dropped to approximately half of its value in 1976 August, and this prevented an accurate position determination.

H_2O 330·88−0·36. This source was discovered independently at Parkes and Itapetinga (Caswell *et al.* 1976; K+ 76, K+ 77) near the position of one of the

strongest known OH masers. The strongest H_2O feature so far observed in this source, at $V = -52\,\mathrm{km\,s^{-1}}$, was found during the first Parkes detection (1975 December), when its peak intensity was ~300 Jy; the intensity fell to ~70 Jy in 1976 August (see Fig. 2) and was below 20 Jy by 1977 May. The other features showed little change between 1976 August and 1977 May. In the Itapetinga measurement of 1975 November the $-51\,\mathrm{km\,s^{-1}}$ feature was $\leqslant 25$ Jy, so that this feature appears to have increased rapidly and declined slowly.

H_2O 330·95−0·19. High-velocity features were detected in 1975 (Goss *et al.* 1976); the more recent spectrum (Fig. 2) shows additional high-velocity features, and it is now one of the most remarkable in appearance, extending to a velocity of $140\,\mathrm{km\,s^{-1}}$ greater than the main features. A spectrum with comparable signal to noise ratio showed no features at more negative velocities.

H_2O 331·13−0·25. This new source is quite weak and has a broad double-peaked velocity structure (Fig. 2). The position is near a new OH source (Caswell *et al.* 1980).

H_2O 331·51−0·10. This is the longest known and strongest southern H_2O source and it is associated with a strong and unusual OH maser; the high-velocity H_2O emission was not discovered until 1975 May and was stronger in 1976 August (Fig. 2) whereas the main emission had weakened.

H_2O 332·65−0·63. The single feature now visible is at a different velocity and is slightly weaker than the peak discovered by K+ 76 and K+ 77. The OH maser detected by Caswell *et al.* (1977) appears not to be closely related, since it is displaced from our H_2O position by several minutes of arc.

H_2O 333·23−0·05. This source was discovered in 1975 November by K+ 76 and K+ 77 near the position of an OH maser (Caswell and Haynes 1975); our 1976 profile (Fig. 2) shows the peak intensity now at the position of a secondary feature of the K+ 77 spectrum, with intensity approximately three times greater.

H_2O 333·13−0·43. Since 1973 June the intensity of the $-51\,\mathrm{km\,s^{-1}}$ peak has declined; other features are now visible (Fig. 2) with our improved sensitivity.

H_2O 333·60−0·22. This is one of the earliest discovered sources; the structure has steadily changed and the peak intensity in 1976 August (Fig. 2) is less than half the maximum recorded value (1973 June).

H_2O 335·78+0·17. This source was discovered in 1976 August near a new OH maser (Caswell *et al.* 1980); the intensity in 1977 May had increased by a factor of 2. A weaker feature (~20 Jy) is present at $-50\,\mathrm{km\,s^{-1}}$.

H_2O 337·40−0·40. This source was discovered in 1975 December (Caswell *et al.* 1976) at the position of an unusual OH source (Caswell *et al.* 1980). The strongest feature of 1975 December was 540 Jy at $V = -43{\cdot}5\,\mathrm{km\,s^{-1}}$ but was not detectable (<15 Jy) in 1976 August, while a secondary feature at $V = -39{\cdot}5\,\mathrm{km\,s^{-1}}$ had decayed from ~50 to ~30 Jy.

H_2O 337·86+0·26. The discovery observation (1975 December) showed a peak of 70 Jy which had fallen to 30 Jy by 1977 May (our next observation, during which a position was measured). The associated OH source has some of the characteristics of a late type OH/IR star (Caswell and Haynes 1975).

H_2O 337·91−0·47. The current peak (Fig. 3) is ~90 Jy at $V = -39$ km s^{-1}, compared with about twice this intensity in 1973 June at a slightly different velocity.

H_2O 338·27+0·54. A single feature of 20 Jy at $V = -56$ km s^{-1} was detected at the discovery epoch (1976 August); by 1977 May a peak at -60 km s^{-1} (not present in 1976) was the strongest feature (see Fig. 3).

H_2O 338·92+0·56. This source was most intense in 1975 November when first discovered (K+ 76); in 1976 August (Fig. 3) the peak intensity of 50 Jy occurred at $V = -75$ km s^{-1} and high-velocity emission was visible at $V = -103$ km s^{-1}. More recently (1977 May) the source was somewhat stronger, with an additional strong (~60 Jy) feature at $V = -54$ km s^{-1} but nothing at $V = -75$ km s^{-1}. Position measurements in 1977 May indicate that the $V = -72$ and -54 km s^{-1} emission comes from the position quoted in Table 2 but that the -64 and -68 km s^{-1} emission is ~20″ arc south of this.

H_2O 340·06−0·25. This source was discovered in 1976 August near the position of an OH maser; no *measurement* of the H_2O position has yet been made (the position listed is that of the OH source).

H_2O 345·41−0·94. This source is near the position of a weak H_2O maser reported by Kaufmann *et al.* (1974). (We are not sure whether it is the same source because Kaufmann *et al.* quoted a very uncertain position and the velocity differs from that of 'our' source.) Our measurements show that the intensity fell ~50% between 1976 August and 1977 May.

H_2O 345·51+0·35. The strong (360 Jy) single feature discovered at $V = -28$ km s^{-1} by K+ 76 was somewhat stronger in 1976 August.

H_2O 345·69−0·09. Two features are visible (Fig. 3) in the 1976 August profile; the peak intensity at many epochs since 1971 has varied by a factor of ~2. The strongest detection so far is 590 Jy (1975 December).

H_2O 348·73−1·04. The peak intensity has increased between the 1975 November discovery (K+ 76) and our 1976 observation (Fig. 3); a weak high-velocity feature is also now visible.

H_2O 349·09+0·11. Between 1975 December and 1976 August (Fig. 4) the feature at $V = -88$ km s^{-1} had decreased by a factor of 2 whereas the feature at -81 km s^{-1} had increased by a factor of ~5.

H_2O 351·16+0·70. High-velocity emission at $V = -80$ km s^{-1}, showing enormous intensity variations (a factor of 5 increase and subsequent decay, all within the period 1976 August 7–10) and a non-detection in 1976 November were reported for this source by Goss *et al.* (1977); in 1977 May we were again unable to detect any high-velocity emission, the only emission being a single feature at $V = -6$ km s^{-1}, which was four times stronger than formerly.

Rodriguez *et al.* (1978) detected highly blue-shifted emission (at $V \sim -80$ km s^{-1}) remarkably similar to that reported by Goss *et al.* (1977) but with position (1950) R.A. $17^h\,16^m\,58^s{\cdot}3$, Dec. $-35°\,51'\,50''$ (with r.m.s. errors ~30″ arc), that is, ~5′ arc from the Goss *et al.* position; the intensity, measured in 1977 November, was ~2300 Jy, or more than 25 times the intensity of the source reported by Goss *et al.*

It is surprising that two such similar and unusual sources should be found in close proximity and the unprecedented short-term intensity variations of one of them are

a further cause for surprise. Application of Occam's razor suggests an alternative explanation which appeals to us but which we have not yet had the opportunity to verify. It seems probable that there are indeed *two low-velocity sources* ($0 \rightarrow -20$ km s^{-1}) at the respective positions listed by Goss *et al.* (1977) and by Rodriguez *et al.* (1978), but that there is only *one high-velocity source* ($V \sim -80$ km s^{-1}), with position as given by Rodriguez *et al.* Goss *et al.* may therefore have detected this high-velocity source in a sidelobe response of their antenna: this would account for their measured intensity being highly variable (due to the shifting pattern of sidelobe responses) and much weaker (<4%) than the Rodriguez *et al.* source. Thus this simple interpretation postulates that (1) there exists one remarkable source rather than two in close proximity and (2) the extremely rapid time variations are not intrinsic to the source but are of instrumental origin.

The association of highly blue-shifted H_2O emission with Herbig–Haro objects was suggested by Rodriguez *et al.* (1978), and the apparently similar source H_2O 291·27−0·71 (see above) may represent the same phenomenon.

H_2O 351·41+0·64. Weak high-velocity emission (at $V = -38$ km s^{-1}) in 1975 May was reported by Goss *et al.* (1976); this was also detected in 1976 August (see Fig. 4). In 1977 May, beyond the negative velocity edge of the main velocity range ($V < -24$ km s^{-1}), an isolated strong feature (~150 Jy) was detected at $V = -33$ km s^{-1} and the highest positive velocity feature was at $V = +4$ km s^{-1} (40 Jy).

H_2O 353·41−0·36. The feature at -14 km s^{-1} (see Fig. 4) increased by a factor of 2·5 between 1976 August and 1977 May whereas near $V = -20$ km s^{-1} the intensity was unchanged.

H_2O 356·64−0·33. This source appears to coincide with IRC–30308, an IR star from which we have detected OH emission. In addition to the feature at $V = -10$ km s^{-1} a slightly weaker feature was detected at -2 km s^{-1}.

H_2O 0·54−0·85. GD 77*a* detected many features in 1976 November spread over the large velocity range 0–90 km s^{-1}. In 1977 May (Fig. 4) we detected an additional feature (25 Jy) at $V = -58$ km s^{-1} so that the mean of the extreme velocities now agrees quite well with the recombination line and OH velocities of ~15 km s^{-1}.

H_2O 5·89−0·40. The strongest feature in this source was at $V = +7$ km s^{-1} in 1975 December (peak of 200 Jy). By 1976 April it had fallen to ~30 Jy and a high-velocity feature at $V = +78$ km s^{-1} was detected with an intensity of ~30 Jy. In 1976 December all intensities remained similar to those of 1976 April (GD 77*a*).

H_2O 12·21−0·11. Our discovery of this unusual source is discussed by Goss *et al.* (1977) and observations have subsequently been reported by GD 77*a*. Our most recent data (1977 May) yield a position (position 1) for the features between -20 and 0 km s^{-1} (as given in Table 2) which agrees more closely with that of GD 77*a* than with the Goss *et al.* (1977) measurement. The feature at $V = +29$ km s^{-1} is displaced to $18^h09^m49^s{\cdot}1$, $-18°25'13''$ (position 2), in good agreement with GD 77*a*. The strongest feature, at $V = +23$ km s^{-1}, is probably at position 1 but may be slightly displaced towards position 2, perhaps as a result of blending. Position 2 is in good agreement with our unpublished OH measurement.

H_2O 12·68−0·18. The major feature showed little change between 1975 December and 1976 December (GD 77*a*).

H_2O 12·91−0·26. The position quoted in Table 2 is the OH position where our measurement was made; GD 77*a* confirm that the accurate H_2O position is very close to this. The single feature decreased by a factor of ~2 between 1976 November (GD 77*a*) and 1977 May.

H_2O 14·17−0·06. Of the four features seen in 1976 August (Fig. 4), the intensity of the one at +61 km s^{-1} had doubled by 1977 May but the others had scarcely changed.

H_2O 14·99−0·69. Our quoted position is taken from Lada *et al.* (1976). Two features, at $V = -4$ and +12 km s^{-1}, detected in 1976 August, were both present in 1976 October (GD 77*a*), one slightly stronger than in August and the other slightly weaker.

H_2O 15·02−0·67. The main features of this source (V between +10 and +21 km s^{-1}) have shown intensity changes of two orders of magnitude since its first discovery (Johnston *et al.* 1973). The source also has high-velocity emission (Goss *et al.* 1976) which GD 77*a* show to be in a position that is significantly displaced (20″ arc) from that of the main source.

H_2O 19·60−0·23. Our measurements of 1975 December and 1976 August show the intensity of features near $V = +40$ km s^{-1} to be ~60 Jy, with a weaker feature at $V = +28$ km s^{-1}; these features are visible in the GD 77*a* data (1976 October) with a more intense sharp feature at $V = +41$ km s^{-1} superposed.

H_2O 24·79+0·08. The intensity was strongest (130 Jy) in our 1975 December observations and dropped to ~70 Jy by 1976 August; GD 77*a* show an intensity that is an order of magnitude weaker for 1976 October but their measurement was apparently made with the source in their principal sidelobe response.

H_2O 30·81−0·06. In our discovery profile (1975 December) the dominant feature was at $V = +82$ km s^{-1} ($S \approx 300$ Jy) with weaker features at +55, +100, +104 and +109 km s^{-1}. For 1976 November the GD 77*a* profile (with better signal to noise ratio than ours) shows emission extending to $V = +125$ km s^{-1} but most features are somewhat weaker.

H_2O 34·25+0·16. Our 1976 August profile shows emission at the same velocities as seen by GD 77*a* in 1976 November; however, in 1976 August all three high-velocity features ($V = +30$, +81 and +87 km s^{-1}) had similar intensities (~30 Jy), giving a much more symmetrical appearance to the profile than was present in the GD 77*a* results.

H_2O 43·80−0·12. The peak intensity of the principal features (near $V = +40$ km s^{-1}) and high-velocity features ($V = +25$, +51 and +56 km s^{-1}) was similar in 1976 August (discovery date), 1977 January (GD 77*a*) and 1977 May, although the structure in most features showed variations; see GD 77*a* for a representative profile.

4. General Discussion

Galactic distribution. It should be noted that although Table 2 provides a comprehensive listing of known H_2O masers close to the galactic plane between longitudes ~200° and 360°, the actual distribution is determined largely by the principal search positions, which were in the directions of known OH masers. Some sources have also been detected by searching in the direction of HII regions. In turn, searches

for OH sources have usually been made at the positions of HII regions. The large number of sources detected between longitudes 326° and 340° is the consequence of an especially intensive OH survey conducted in this region.

Sources with no accompanying OH maser. An important survey has been conducted at Itapetinga in which HII regions without any known OH masers have been searched for H_2O; several successful detections have resulted. We have subsequently searched for weak OH masers in these directions and in several cases have found an OH counterpart (Haynes *et al.* 1976; Caswell *et al.* 1977); we have argued that the absence of an OH maser is not evidence of any different population of H_2O masers, but nonetheless this class of H_2O source merits particularly detailed investigation.

Polarization. As noted in Section 2 above, linear polarization data on many of the individual sources at a single epoch are presented by Knowles and Batchelor (1978).

Velocity structures and high velocity features. The range of velocity structures encountered in different sources is quite varied, as can be seen from Figs 1–4. Most commonly (e.g. $H_2O\,291{\cdot}57-0{\cdot}43$, $305{\cdot}20+0{\cdot}21$, $305{\cdot}36+0{\cdot}15$, $330{\cdot}88-0{\cdot}36$ etc.) several strong features occur over a velocity range of $\sim 20\,km\,s^{-1}$, centred approximately on the velocity of an associated HII region and OH maser. In some cases (e.g. $H_2O\,330{\cdot}95-0{\cdot}19$, $331{\cdot}51-0{\cdot}10$) additional H_2O features are present, displaced in velocity by amounts which sometimes exceed $100\,km\,s^{-1}$; these are usually referred to as 'high-velocity features' and it is now clear (see also Goss *et al.* 1976) that their occurrence is quite common—certainly not a rare phenomenon confined to a few powerful sources, as was once thought to be the case.

Early work suggested that high-velocity features were invariably weaker than emission from the 'main' velocity range, but this is not the case in several examples reported by Goss *et al.* (1977). Rodriguez *et al.* (1978) found two examples of intense high-velocity H_2O emission at the positions of Herbig–Haro objects. As remarked in our notes to $H_2O\,291{\cdot}27-0{\cdot}71$ and $H_2O\,351{\cdot}16+0{\cdot}70$ in Section 3 above, the sources reported by Goss *et al.* (1977) may also fit this proposed association of particularly intense high-velocity H_2O emission with Herbig–Haro objects.

In a simple model to account for the Orion nebula H_2O emission, Genzel and Downes (1977*b*) distinguish between an expanding shell of emission (actually two nearby shells) accounting for the strong central features and high-velocity fragments accelerated by a stellar wind. (The shell model has, of course, also been used to account for the structure of both the OH and H_2O masers in VY CMa and the late-type stars.) GD 77*a* suggest that similar distinctions apply to other sources. While their model is helpful in understanding the Orion H_2O emission there are many sources which cannot easily be fitted into this scheme. The unusual high-velocity sources discussed by Goss *et al.* (1977) are particularly difficult to account for, since the high-velocity emission is much stronger than the main 'shell' emission. There are also sources, such as $H_2O\,0{\cdot}54-0{\cdot}85$ (Fig. 4), where it is difficult to decide whether the structure is better described as resulting from widely separated shells, or as central emission with strong high-velocity features.

Mapping of more sources with adequate spatial resolution may shed light on this problem in the future, although in cases where this has already been done the interpretation is *still* not clear. For example, in Orion A the fragments with highest *radial* velocity tend to be furthest from the main features of emission; contrary to the

remarks of Genzel and Downes (1977*b*), it is not clear why this should be expected from their model.

It has been noted in the past that there is a tendency for high-velocity features to be more numerous at negative velocities than at positive velocities; with our discovery of more examples of high-velocity emission this effect is still noticeable but its statistical significance is still not certain. There are certainly individual sources where only *positive* high-velocity features are seen, and others where the emission is fairly symmetrical about the main features.

Spatial structure. In a number of sources, emission has been detected from several spatially separated positions. In some cases, the high-velocity features are separated from the low-velocity emission. An important question is whether the source of excitation, the maser pump, is internal to each of these spatially separate components; the answer is still not clear.

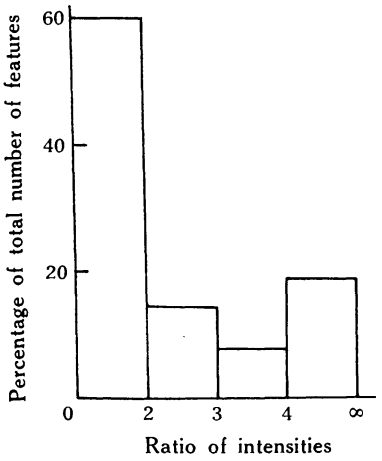

Fig. 5. Variability of H_2O maser features over an 8 month interval. The majority of features show little change, while a small proportion exhibit extreme variations.

Variability. Although a few sources have previously been studied in detail for variability, the present data are complementary, in that it can be seen: (1) how commonly we find *extreme* variability (e.g. an order of magnitude); (2) whether the extreme variability is confined to a few features in multifeature sources; (3) whether the variability of high-velocity features is generally more extreme than that of the main features.

We have analysed the distribution function of different intensity changes which take place in an 8 or 9 month interval, and the histogram of Fig. 5 summarizes the result. This shows that, on the average, slightly more than half of the features seen at one epoch are present 8 months earlier or later with an intensity differing by less than a factor of 2 (either increase or decrease); approximately one-sixth will differ by more than a factor of 4 (increase or decrease). This can be used as a comparison standard for studying the high-velocity features and multifeature sources when more statistics are available. At present the indications are that in multiple feature sources, some sources *as a whole* can be categorized as more (or less) variable than average and that high-velocity features are somewhat more highly variable than those in the main velocity range.

5. Conclusions

The present study has provided a large sample of sources which now need to be investigated in more detail; the number of sources displaying high-velocity features is now considerable and it will be important to ascertain how commonly these are displaced spatially from the main velocity range and to what extent they fit into the scheme proposed by GD 77*a*; essentially the question remains: are many of the sources similar to Orion and perhaps even to VY CMa and are there only a few centres of excitation in each 'cluster'?

Complementary observations are now needed to search for possible counterparts to the H_2O masers in the IR range and in the radio continuum at high frequencies.

References

Caswell, J. L., *et al.* (1976). *Proc. Astron. Soc. Aust.* **3**, 61.
Caswell, J. L., Batchelor, R. A., Haynes, R. F., and Huchtmeier, W. K. (1974). *Aust. J. Phys.* **27**, 417.
Caswell, J. L., and Haynes, R. F. (1975). *Mon. Not. R. Astron. Soc.* **173**, 649.
Caswell, J. L., Haynes, R. F., and Goss, W. M. (1977). *Mon. Not. R. Astron. Soc.* **181**, 427.
Caswell, J. L., Haynes, R. F., and Goss, W. M. (1980). A survey of OH masers at 1665 and 1667 MHz. I. Galactic longitudes 326° to 340°. *Aust. J. Phys.* (in press).
Genzel, R., and Downes, D. (1977*a*). *Astron. Astrophys. Suppl.* **30**, 145.
Genzel, R., and Downes, D. (1977*b*). *Astron. Astrophys.* **61**, 117.
Goss, W. M., Haynes, R. F., Knowles, S. H., Batchelor, R. A., and Wellington, K. J. (1977). *Mon. Not. R. Astron. Soc.* **180**, 51P.
Goss, W. M., Knowles, S. H., Balister, M., Batchelor, R. A., and Wellington, K. J. (1976). *Mon. Not. R. Astron. Soc.* **174**, 541.
Haynes, R. F., Caswell, J. L., and Goss, W. M. (1976). *Proc. Astron. Soc. Aust.* **3**, 57.
Johnston, K. J., Sloanaker, R. M., and Bologna, J. M. (1973). *Astrophys. J.* **182**, 67.
Kaufmann, P., *et al.* (1976). *Nature* **360**, 306.
Kaufmann, P., Fogarty, W. G., Scalise, E., and Schaal, R. E. (1974). *Astron. J.* **79**, 933.
Kaufmann, P., Zisk, S., Scalise, E., Schaal, R. E., and Gammon, R. H. (1977). *Astron. J.* **82**, 577.
Knapp, G. R., and Morris, M. (1976). *Astrophys. J.* **206**, 713.
Knowles, S. H., and Batchelor, R. A. (1978). *Mon. Not. R. Astron. Soc.* **184**, 107.
Lada, C. J., Dickinson, D. F., Gottlieb, C. A., and Wright, E. L. (1976). *Astrophys. J.* **207**, 113.
Rodriguez, L. F., Moran, J. M., Dickinson, D. F., and Gyulbudaghian, A. L. (1978). *Astrophys. J.* **226**, 115.
Scalise, E., and Schaal, R. E. (1977). *Astron. Astrophys.* **57**, 475.

Manuscript received 14 May 1979